Available online at www.sciencedirect.com
SCIENCE DIRECT
International Journal of Heat and Mass Transfer 49 (2006) 3253–3263
International Journal of HEAT and MASS TRANSFER
www.elsevier.com/locate/ijhmt

An analytical solution for the stationary behaviour of binary mixtures and pure fluids in a horizontal annular cavity

G. Desrayaud [a,1], A. Fichera [b,*], M. Marcoux [a,1], A. Pagano [b]

[a] INSSET, LETEM, Université de Picardie Jules Verne, 48 Rue Raspail BP 422 02109, Saint-Quentin, France
[b] DIIM, Università degli Studi di Catania, Viale Andrea Doria 6, 95125 Catania, Italy

Received 20 September 2005
Available online 29 March 2006

Abstract

This study aims at analysing the characteristics of the two-dimensional flow established by binary mixtures and pure fluids in a horizontal annular cavity isothermally heated inside and cooled outside. Some complications arise considering binary mixtures, as a consequence of thermogravitational diffusion due to the coupling of convection with thermodiffusion.

An analytical model has been defined assuming a two-dimensional laminar flow of a visco-elastic fluid, under validity of Boussinesq's assumption and negligible viscous dissipation. For the case of binary mixtures, the buoyancy determined by concentration variations has been ignored, so that momentum equation is independent on concentration and is only coupled with the energy balance equation.

The analytical model has been validated, for both cases of binary mixtures and pure fluids, through comparison with numerical results in a wide range of the non-dimensional parameters that govern the problem. In particular, the effect of the geometry and of the boundary conditions on the separation of the mixture compounds due to thermogravitational diffusion has been exploited.

Keywords: Thermogravitation; Binary mixtures; Annular cavity; Analytical solution; Numerical model

1. Introduction

The evaluation of heat and mass transfer in natural convection-based systems and their description through appropriate models generally represent complex problems, due both to the high order of the system and to the existence of several non-linear couplings between the system variables. The definition of analytical solutions is sometimes possible under restrictive geometrical and thermal–fluidynamic conditions, with the main advantage of generality within the range of validity of the assumed restrictions. On the other hand, in most cases numerical models can be properly adopted with minor restrictions but with lost of flexibility, as a specific numerical model must be implemented for each operating condition and for each geometrical configuration.

This study addresses the problem of defining an analytical model able to describe heat and mass transfer phenomena occurring in a horizontal annular cavity delimited by two isothermally and differentially heated concentric cylinders. Two different kinds of fluid have been considered: (a) binary mixtures and (b) pure fluids. The case of pure fluids can be considered as a restriction of the more complex case of binary mixtures. The last are, in fact, subjected not only to natural convection but also to the mechanism of thermodiffusion (also known as Soret effect) [1], i.e. the generation of a concentration gradient in presence of a thermal gradient, with separation of the mixture compounds. The coupling of the two mechanisms is called thermogravitational diffusion and, under appropriate circumstances, can sensibly enhance compound separation with respect to thermodiffusion [2].

This kind of phenomenon has been reported in several analytical and numerical studies, for rectangular [2] or

* Corresponding author. Tel.: +39 095 7382450; fax: +39 095 7382496.
E-mail addresses: gilles.desrayaud@insset.u-picardie.fr (G. Desrayaud), afichera@diim.unict.it (A. Fichera).
[1] Tel.: +33 3 23 628959; fax: +33 3 23 628935.

0017-9310/$ - see front matter © 2006 Elsevier Ltd. All rights reserved.
doi:10.1016/j.ijheatmasstransfer.2006.02.002

Nomenclature

a thermal diffusivity
C concentration
$C' = \frac{C-C_0}{\Delta C}$ non-dimensional concentration
$\Delta C = N\frac{\beta_0}{\gamma_0}\Delta T$ reference concentration difference
D mass diffusion coefficient
$e = r_e - r_i$ dimensional gap width
g gravity
$Gr = \frac{g\beta(T_i-T_0)L_i^3}{\nu_0^2}$ Grashof number
$Le = \frac{a_0}{D}$ Levis number
$N = \frac{\gamma_0}{\beta_0}\frac{\Delta C}{\Delta T}$ non-dimensional parameter
p pressure
$p' = \frac{p}{\rho_0 V_0^2}$ non-dimensional pressure
$Pr = \frac{\nu_0}{a_0}$ Prandtl number
r radius
$r' = \frac{r}{e}\, r' \in \left[\frac{1}{R-1}; \frac{R}{R-1}\right]$ non-dimensional radius
$R = \frac{r_e}{r_i}$ radius ratio
t dimensional time
$t' = \frac{a_0 t}{e^2}$ non-dimensional time
$Ra = Gr \cdot Pr$ Rayleigh number
$S_T = \frac{D_T}{D}\frac{(T_i-T_0)}{\Delta C}$ Soret number
T dimensional temperature
$T_0 = \frac{T_i+T_e}{2}$ mean (reference) temperature
$\Delta T = T_e - T_i$ temperature difference
$T' = \frac{T-T_0}{\Delta T}$ non-dimensional temperature
u dimensional radial velocity
$u' = u/V_0$ non-dimensional radial velocity
$V_0 = \frac{a_0}{e}$ dimensional reference velocity
v dimensional tangential velocity
$v' = v/V_0$ non-dimensional tangential velocity

Greek symbols
β thermal expansion coefficient
γ mass expansion coefficient
μ dynamic viscosity
ν cinematic viscosity
ρ density

Subscripts
e external
i internal
0 reference value\

cylindrical cavities [3] vertically displaced, with and without a porous medium filling it [4]. For both these configurations, the stationary behaviour in presence of a horizontal thermal gradient is characterised by a vertical stratification of the concentration field, with accumulation regions for the two compounds placed at the bottom and top of the cavity. The rate of separation varies with geometrical and boundary conditions and can be considerable at the optimal situation.

For what concern natural convection in the horizontal annular cavity, several experimental and theoretical studies have been reported, due to the relevant interest towards this configuration in various technical and industrial heat transfer problems, such as transmission cables, latent energy storage systems, components of nuclear reactors, etc. The behaviour of binary mixtures in horizontal annular cavities, complicated by the contemporary presence of natural convection and Soret effect, has not yet been exploited.

The non-dimensional analytical model defined in this study aims at describing the two-dimensional temperature, velocity and concentration profiles that, under some restrictive assumptions, characterise the behaviour of a binary mixtures filling a horizontal annular cavity isothermally heated inside and cooled outside. Once that such an analytical model has been defined, the analogous description for pure fluids simply represents a restriction of that of binary mixtures, through the elimination of concentration.

For both cases of pure fluid and binary mixtures, the basic assumptions considered in order to define the analytical model are:

- visco-elastic fluid,
- laminar and two-dimensional flow,
- validity of Boussinesq's hypothesis,
- negligible viscous dissipation.

Moreover, the mass flux determined by the concentration-driven buoyancy term has been neglected for the case of binary mixtures, allowing to decouple momentum equation from the dependence on concentration. In this way it is possible to solve the analytical problem in two steps: at first, the coupled thermal and velocity fields can be analytically determined, then it is possible to define an analytical equation for the concentration field.

The second fundamental assumption consists in considering a pseudo-conductive regime inside the cavity, i.e. a temperature distribution inside the cavity that is characterised by cylindrical isotherms, for which conduction represents the major mode for heat transfer. This regime has been experimentally observed and described in [5], and consists of two crescent-shaped cells, symmetrical with respect to the cavity vertical axis, as described numerically in [6]. The fluid in contact with the hot inner cylinder rises following an upward trajectory, reaches the top of the annulus and then goes down along a trajectory approximately parallel to the outer cylindrical surface. Over a certain Rayleigh number, dependent on the geometry, this regime is disrupted:

- at high radius ratio, by a thermal plume that originates at the top of the annulus,

- at low radius ratio, for the birth of a multicellular flow pattern of the Rayleigh–Bénard type [6–9], initially characterised by two small cells at the top of the annulus (in addition to the crescent-shaped cells occupying the whole annulus in the former pseudo-conductive regime).

In both cases, as the Rayleigh number is further increased, these structures undergo several bifurcations due to the birth of complex flow structures [10].

The following sections describe the approach used to define the analytical solutions for binary mixtures and for pure fluids. Moreover, the analytical results are compared with those obtained by a widely tested numerical model, in order to assess the ranges of the non-dimensional parameters for which the analytical model satisfactorily predicts the behaviour of the system.

2. Problem statement

Consider the horizontal annular cavity formed by the two infinite long concentric cylinders of radius r_i and r_0 shown in Fig. 1.

This study aims at describing the behaviour of either binary mixtures or pure fluids filling the cavity, for the case of isothermal cylindrical walls at different imposed temperatures. In particular, the case of isothermally heated inner cylinder and isothermally cooled outer cylinder, i.e. $T_i > T_e$, has been herein considered; the inverse thermal condition can be easily deduced from the results reported in the following.

For both binary mixtures and pure fluids, the fluid filling the cavity has been supposed incompressible and newtonian, with dynamic viscosity μ. Moreover, as the focus of this study is on the convective behaviour, usually characterised by low flow velocity, the three-dimensional complex motions that can arise along the annulus axial coordinate have been neglected, i.e. the flow has been assumed two-dimensional and laminar. In accordance with Boussinesq's hypothesis, the variations of the fluid density ρ are neglected in all terms except in the buoyancy, in which it is supposed to depend linearly on both temperature and concentration, i.e. $\rho = \rho_0(1 - \beta_0(T - T_0) + \gamma_0(C - C_0))$, with β_0 and γ_0 coefficients of thermal and mass expansion respectively.

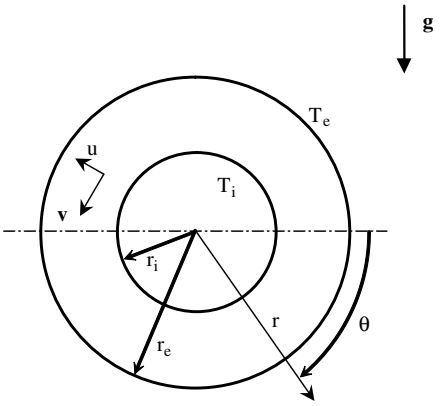

Fig. 1. Schematic of the annular cavity with imposed wall temperatures.

Finally, neglecting the energy dissipated by viscous stresses, the mass, momentum (along r and θ), energy and concentration balance equations can be written as

$$\frac{1}{r}\frac{\partial}{\partial r}(ru) + \frac{1}{r}\frac{\partial}{\partial \theta}(v) = 0 \tag{1}$$

$$\rho_0\left(\frac{\partial u}{\partial t} + u\frac{\partial u}{\partial r} + \frac{v}{r}\frac{\partial u}{\partial \theta} - \frac{v^2}{r}\right) = -\frac{\partial p}{\partial r} - \rho_0 g[\beta_0(T - T_0) + \gamma_0(C - C_0)]\sin\theta + \mu_0\left(\frac{1}{r}\frac{\partial}{\partial r}\left[r\frac{\partial u}{\partial r}\right] + \frac{1}{r^2}\frac{\partial}{\partial \theta}\left[\frac{\partial u}{\partial \theta}\right] - \frac{2}{r^2}\frac{\partial v}{\partial \theta} - \frac{u}{r^2}\right) \tag{2}$$

$$\rho_0\left(\frac{\partial v}{\partial t} + u\frac{\partial v}{\partial r} + \frac{v}{r}\frac{\partial v}{\partial \theta} + \frac{uv}{r}\right) = -\frac{1}{r}\frac{\partial p}{\partial \theta} + \rho_0 g[\beta_0(T - T_0) + \gamma_0(C - C_0)]\cos\theta + \mu_0\left(\frac{1}{r}\frac{\partial}{\partial r}\left[r\frac{\partial v}{\partial r}\right] + \frac{1}{r^2}\frac{\partial}{\partial \theta}\left[\frac{\partial v}{\partial \theta}\right] + \frac{2}{r^2}\frac{\partial u}{\partial \theta} - \frac{v}{r^2}\right) \tag{3}$$

$$\frac{\partial T}{\partial t} + u\frac{\partial T}{\partial r} + \frac{v}{r}\frac{\partial T}{\partial \theta} = a_0\left(\frac{1}{r}\frac{\partial}{\partial r}\left[r\frac{\partial T}{\partial r}\right] + \frac{1}{r^2}\frac{\partial}{\partial \theta}\left[\frac{\partial T}{\partial \theta}\right]\right) \tag{4}$$

$$\rho_0\left(\frac{\partial C}{\partial t} + u\frac{\partial C}{\partial r} + \frac{v}{r}\frac{\partial C}{\partial \theta}\right) = \rho_0 D\left(\frac{1}{r}\frac{\partial}{\partial r}\left[r\frac{\partial C}{\partial r}\right] + \frac{1}{r^2}\frac{\partial^2 C}{\partial \theta^2}\right) + \rho_0 D_T\left(\frac{1}{r}\frac{\partial}{\partial r}\left[r\frac{\partial T}{\partial r}\right] + \frac{1}{r^2}\frac{\partial^2 T}{\partial \theta^2}\right) \tag{5}$$

where the Doufur effect has been neglected. This means that the heat flux determined by concentration gradients is ignored [4]. Eqs. (1)–(5) can be rewritten in the following no-dimensional form:

$$\frac{\partial ru}{\partial r} + \frac{\partial v}{\partial \theta} = 0 \tag{6}$$

$$\frac{\partial u}{\partial t} + u\frac{\partial u}{\partial r} + \frac{v}{r}\frac{\partial u}{\partial \theta} - \frac{v^2}{r} = -\frac{\partial p}{\partial r} - Ra\,Pr\sin\theta(T + NC) + Pr\left[\frac{1}{r}\frac{\partial}{\partial r}\left(r\frac{\partial u}{\partial r}\right) + \frac{1}{r}\frac{\partial}{\partial \theta}\left(\frac{\partial u}{\partial \theta}\right) - \frac{2}{r^2}\frac{\partial v}{\partial \theta} - \frac{u}{r^2}\right] \tag{7}$$

$$\frac{\partial v}{\partial t} + u\frac{\partial v}{\partial r} + \frac{v}{r}\frac{\partial v}{\partial \theta} + \frac{uv}{r} = -\frac{1}{r}\frac{\partial p}{\partial \theta} + Ra\,Pr\cos\theta\,(T + NC) + Pr\left[\frac{1}{r}\frac{\partial}{\partial r}\left(r\frac{\partial v}{\partial r}\right) + \frac{1}{r^2}\frac{\partial}{\partial \theta}\left(\frac{\partial v}{\partial \theta}\right) + \frac{2}{r^2}\frac{\partial u}{\partial \theta} - \frac{v}{r^2}\right] \tag{8}$$

$$\frac{\partial T}{\partial t} + u\frac{\partial T}{\partial r} + \frac{v}{r}\frac{\partial T}{\partial \theta} = \frac{1}{r}\frac{\partial}{\partial r}\left(r\frac{\partial T}{\partial r}\right) + \frac{1}{r^2}\frac{\partial}{\partial \theta}\left(\frac{\partial T}{\partial \theta}\right) \tag{9}$$

$$\frac{\partial C}{\partial t}+u\frac{\partial C}{\partial r}+\frac{v}{r}\frac{\partial C}{\partial \theta}=\frac{1}{Le}\left(\frac{1}{r}\frac{\partial}{\partial r}\left[r\frac{\partial C}{\partial r}\right]+\frac{1}{r^2}\frac{\partial^2 C}{\partial \theta^2}\right)+\frac{1}{Le}S_T\left(\frac{1}{r}\frac{\partial}{\partial r}\left[r\frac{\partial T}{\partial r}\right]+\frac{1}{r^2}\frac{\partial^2 T}{\partial \theta^2}\right) \quad (10)$$

The boundary conditions for these equations express the conditions of isothermal walls, null velocity at the walls and impermeable walls, therefore

$$T|_{r_i}=0.5; \quad T|_{r_e}=-0.5 \quad (11)$$

$$u,v|_{r_i}=0; \quad u,v|_{r_e}=0 \quad (12)$$

$$\left(\frac{\partial C}{\partial r}=-\frac{1}{S_T}\frac{\partial T}{\partial r}\right)_{r_i}; \quad \left(\frac{\partial C}{\partial r}=-\frac{1}{S_T}\frac{\partial T}{\partial r}\right)_{r_e} \quad (13)$$

3. Numerical resolution

Model (6)–(10) has been numerically solved by means of a finite element code, which has been widely validated [6,10]. The system geometry, characterised by the radius ratio $R=r_e/r_i(R\in]1;+\infty[)$, is defined by the domain $(r,\theta)\in[r_i=1/(R-1),\ r_e=R/(R-1)]\times[0,2\pi]$. The domain has been discretised using a unstructured triangular grid having 1000 nodes (1808 triangles). A first-order implicit scheme has been adopted for the temporal resolution of the discretised equations, whereas the pressure–velocity coupling has been solved by means of the improved Lagrangian algorithm in association with the penalisation method. The integration of momentum, energy and concentration balance equations has been performed by direct matrix resolution (LU factorisation).

Calculations have been performed using primitive variables; nonetheless, in the following also the streamfunction ψ has been used for the presentation of results. The streamfunction has been defined as the function respecting the following conditions:

$$u=\frac{1}{r}\frac{\partial \psi}{\partial \theta}; \quad v=-\frac{\partial \psi}{\partial r} \quad (14)$$

For the definition of the numerical model, a binary mixture has been assumed to fill the cavity. In particular, a H_2O–C_3H_8O (water–isopropanol) mixture with 50% in mass of both constituents has been considered. Moreover, the numerical resolution has been applied to a cavity with radius ratio $R=1.5$ and considering a set of boundary conditions for which thermogravitation can be experimentally observed.

Thermo-physical properties of the mixture are reported in Table 1 together with the chosen boundary conditions and the corresponding non-dimensional parameters.

The simulation of the numerical model for the previous case yields to the stationary behaviour corresponding to the temperature and concentration fields and to the streamfunction reported in Fig. 2.

In Fig. 2(a) it is possible to observe that the stationary temperature field is characterised by a concentric distribution of the isotherms strongly resembling that of the conductive regime and called, therefore, pseudo-conductive. For this regime, the flow inside the cavity is separated in two distinct counterotating cells that are symmetrical with respect to the vertical axis of the cavity, as indicated by the streamfunction distribution reported in Fig. 2(b). For this kind of flow the two components of the velocity vector $\boldsymbol{V}=(u(r,\theta),(v(r,\theta))$ are sensibly different at any angular location in the annulus except in the regions around $\theta=-\pi/2$ and $\theta=+\pi/2$ (i.e. the regions in which the cells are in contact with each other). In fact, the radial velocity component, u, is much smaller than the component in the tangential direction, v; moreover, v strongly depends on θ, whereas only marginally on r.

The distribution that characterises the concentration field can be observed in Fig. 2(c). This field shows a vertical stratification with the two compounds separating respectively at the top and the bottom of the annulus; moreover,

Table 1
Dimensional and non-dimensional parameters considered during numerical simulations

β (K^{-1})	γ	a_0 ($m^2\,s^{-1}$)	μ ($kg\,m^{-1}\,s^{-2}$)	ρ ($kg\,m^{-3}$)	D ($m^2\,s^{-1}$)	D_T ($m^2\,s^{-1}\,K^{-1}$)	C_0	ΔT (K)	L (mm)
7.7×10^{-4}	−0.25	1.0×10^{-7}	3.08×10^{-3}	905	10^{-9}	5×10^{-12}	0.5	−10 K	0.5
$Ra=27.6$		$Pr=33.9$		$N=-1.62$		$Le=100$		$R=1.5$	

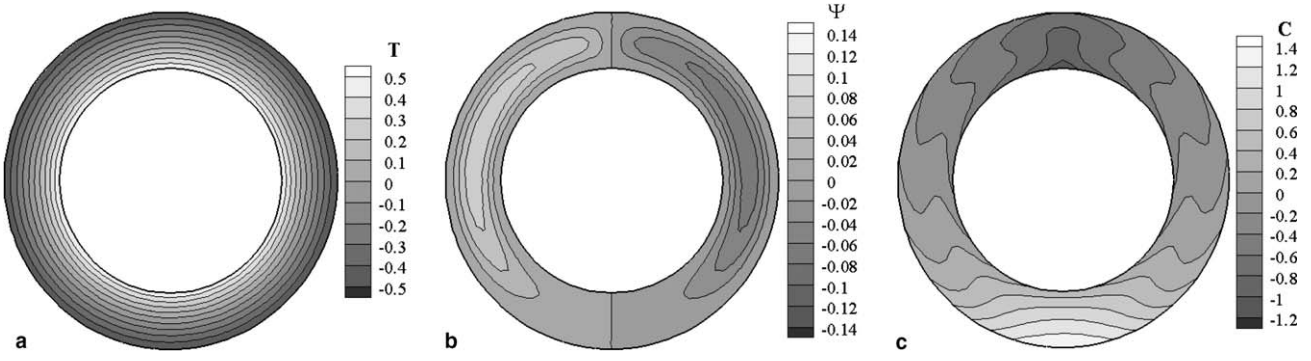

Fig. 2. Numerical results: (a) temperature, (b) streamfunction and (c) concentration fields.

the degree of separation is higher than that due exclusively to the pure Soret effect.

The physical meaning of previous results does not change with the inversion of the temperature gradient; simply, the temperature and velocity fields will be the inverse of those reported in Fig. 2(a) and (b), whereas the concentration field will be inverted with respect to the horizontal axis.

4. Analytical model

Previous considerations are fundamental for the possibility they give to simplify the problem in view of the definition of an analytical solution, similarly to what has been done for the simpler cases of rectangular or cylindrical cavities [2,3]. The following simplifications have been considered valid for the description of the stationary behaviour:

- temperature distribution corresponds to that of the pure conductive regime, therefore, $T(r,\theta) \cong T(r)$,
- the radial component of the velocity can be neglected with respect to the tangential component, which depends only on r; therefore, $V = (u(r,\theta),\ v(r,\theta)) \cong V = (0, v(r))$,
- the velocity field is influenced only by the temperature gradient, and the effect of the concentration can be neglected; therefore (namely, *forgotten effect*), $T \gg NC \approx 0$,
- the concentration field can be considered linearly stratified along the tangential direction θ, therefore, $C(r,\theta) = \varphi(r) + b\theta$.

Hence, the following simplified non-dimensional model can be considered for the regime condition:

$$-\frac{v^2}{r} = -\frac{\partial P}{\partial r} - Ra\,Pr\,T\sin\theta \tag{15}$$

$$0 = -\frac{1}{r}\frac{\partial P}{\partial \theta} + Ra\,Pr\,T\cos\theta + Pr\left[\frac{1}{r}\frac{\mathrm{d}}{\mathrm{d}r}\left(r\frac{\mathrm{d}v}{\mathrm{d}r}\right) - \frac{v}{r^2}\right] \tag{16}$$

$$0 = \frac{1}{r}\frac{\mathrm{d}}{\mathrm{d}r}\left(r\frac{\mathrm{d}T}{\mathrm{d}r}\right) \tag{17}$$

$$\frac{v}{r}b = \frac{1}{Le}\left[\frac{\partial^2\varphi}{\partial r^2} + \frac{1}{r}\frac{\partial\varphi}{\partial r}\right] \tag{18}$$

It is worth noting that, not depending on v and C, Eq. (17) is decoupled from the other equations. Moreover, the subsystem formed by Eqs. (15)–(17) is decoupled from Eq. (18) and can be separately solved; at the same time, this subsystem represents the restriction of the problem to the case of pure fluid filling the annulus. This means that the temperature and velocity fields determined from this subset of equations are valid for both binary mixtures and pure fluids.

Double integration of Eq. (17) yields

$$T(r) = C_1\ln(r) + C_2 \tag{19}$$

with integration constants C_1 and C_2 to be determined by imposing at the boundaries thermal conditions (11). This leads to

$$T(r) = 0.5 - \frac{\ln(r) + \ln(R-1)}{\ln(R)} \tag{20}$$

Eq. (20) describes the temperature profile for the pseudo-conductive regime in a horizontal cylindrical cavity filled either by a binary mixture or by a pure fluid. It is important to observe that the analytical solution depends only on the geometry, characterised by the radius ratio R, and by the radial position at which the temperature profile is evaluated; it does not depend on the angular position θ (as a consequence of the assumption of concentric cylindrical isotherms) nor on the value of Ra.

Once that the temperature profile has been found, it is possible to find the corresponding velocity profile. In order to do so, it is convenient to differentiate Eqs. (15) and (16) with respect to θ and r respectively and subtract them from one another. This results in the following third order ordinary differential equation:

$$\frac{\mathrm{d}^3 v}{\mathrm{d}r^3} + \frac{2}{r}\frac{\mathrm{d}^2 v}{\mathrm{d}r^2} - \frac{1}{r^2}\frac{\mathrm{d}v}{\mathrm{d}r} + \frac{v}{r^3} + Ra\sin\theta\frac{\partial T}{\partial r} = 0 \tag{21}$$

Eq. (21) can be numerically integrated for specified values of R and Ra considering boundary conditions expressed by (12) and an additional condition, which can be found in the application of conservation of mass over the horizontal section (at $\theta = 0$)

$$\int_{r_i}^{r_e} v(r)\,\mathrm{d}r = 0 \tag{22}$$

In this way the velocity profile for the pseudo-conductive regime is determined in the form

$$v(r) = \frac{Ra\sin\theta}{3\ln(R)}r^2 + C_3 r + \frac{C_4}{r} + C_5 r\ln(r) \tag{23}$$

It is worth noting that integration constants C_3, C_4 and C_5 in Eq. (23) are numerically obtained; therefore they assume values to be determined for each couple of R and Ra values.

Eqs. (20) and (22) constitute the analytical solution approximating the thermal and fluidynamic fields for a horizontal annular cavity isothermally heated inside and cooled outside, both for the case of binary mixtures and for that of pure fluids. It is worth noting that, though this solution indirectly depends on Pr through the Rayleigh number, it does not directly depend on it, as a consequence of the assumptions of stationary behaviour and r-stratified θ-independent velocity distribution.

Finally, now that the analytical velocity profile is known, it can be substituted in Eq. (18). The obtained equation can be numerically integrated by imposing the boundary conditions on the concentration expressed in (13) and the following supplementary integral condition of conservation of the total amount of solutal inside the cavity

$$\int\int_V \varphi(r,\theta) r\,\mathrm{d}\theta\,\mathrm{d}r = C_0 \tag{24}$$

This yields the following form of the analytical concentration profile:

$$\varphi(r) = bLe\left[\frac{Ra\sin\theta}{27\ln(R)}r^3 + \frac{C_3}{4}r^2 + \frac{C_4}{2}\ln(r)^2 + \frac{C_5}{4}r^2(\ln(r)-1)\right] + C_6\ln(r) + C_7 \quad (25)$$

Again, as for the case of the velocity profile, the integration constants C_6 and C_7 are numerically determined.

The last constant to be determined for the closure of the concentration problem is the one expressing the stratification of the concentration, i.e. b. This constant can be obtained by imposing an additional equilibrium condition for the stationary state, i.e. the balance between the diffusive and convective terms of transport of the solutal through the horizontal section ($\theta = 0$)

$$\int_{r_i}^{r_e} v(r)C(r)r\,dr = \frac{b}{Le} \quad (26)$$

In this way, also the analytical solution for the concentration field inside the cavity $C(r,\theta)$ can be completely determined.

The analytical profiles of temperature, velocity and concentration for the same binary mixture considered for the calculation of the numerical profiles previously described are reported in Fig. 3 for a semiannulus. The comparison of these profiles with those reported in Fig. 3 points out the capability of the analytical model to satisfactorily describe the three fields everywhere except that at the top and the bottom of the annulus, as expected from simplifications at the basis of the analytical solution. In these regions, in fact, the analytical velocity does not account for the velocity reduction, originated by the actual separation of the flow in two convective cells, which, instead, is revealed by the numerical model. As a consequence, at the top and the bottom of the annulus the analytical concentration profile is not affected by this velocity reduction and therefore is not deformed. Nonetheless, the analytical and numerical concentration profiles are indeed very similar and present, in the overall, the same component separation of the binary mixture.

5. Numerical validation of the analytical model

In order to validate the analytical model, its results have been compared with those obtained by the numerical model previously described in a wide range of both Ra and R.

Different comparisons have been performed, depending on the kind of fluid filling the annular cavity (i.e. binary mixtures or pure fluids). In particular:

- for both binary mixtures and pure fluids, the capability of the analytical model to reproduce the numerical profiles has been analysed,
- for the case of binary mixtures, special attention has been devoted to the influence of Ra and R on the separation of the mixture compounds, due to the industrial relevance of this effect,
- for the case of pure fluids, the interest has been concentrated on the capability of the analytical model to predict the heat transfer, through the comparison of the analytical and numerical Nusselt number.

5.1. Binary mixtures

For this case, the analytical solution has been compared versus the numerical model varying both Ra and R and maintaining constant all the other parameters, at typical values of several liquid binary mixtures ($Pr = 10$, $NC \approx 0$, $Le = 100$).

Fig. 4 reports the comparison of the temperature, velocity and concentration profiles evaluated at $\theta = 0$ for $Ra = 100$ and various R. Also the case $R = 1$ is reported in the plots, which represents the case of infinite curvature of the cavity, i.e. the extrapolation of the results obtained for the rectangular geometry in cartesian geometry in a previous study [2].

The analysis of the plots shows the satisfactory capability of the analytical solution of reproducing the numerical profile taken as reference for the whole range of parameters. In particular, it is worth noting that also the analytical profiles tend to loose symmetry with the increase of the

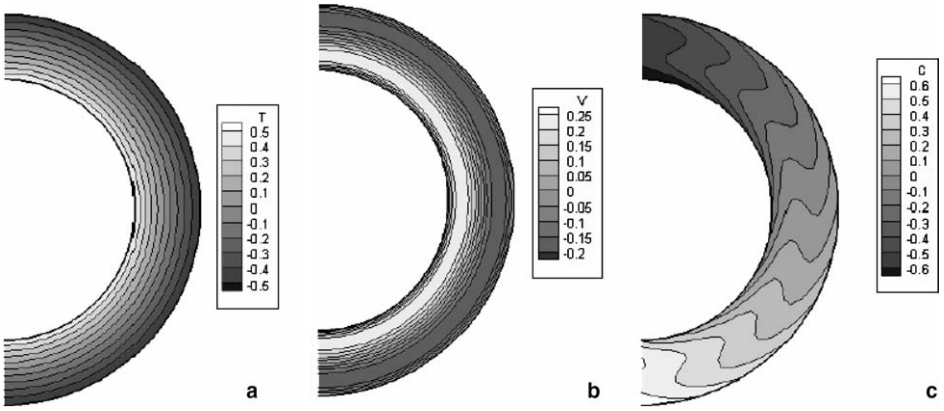

Fig. 3. Analytical results: (a) temperature, (b) velocity and (c) concentration fields.

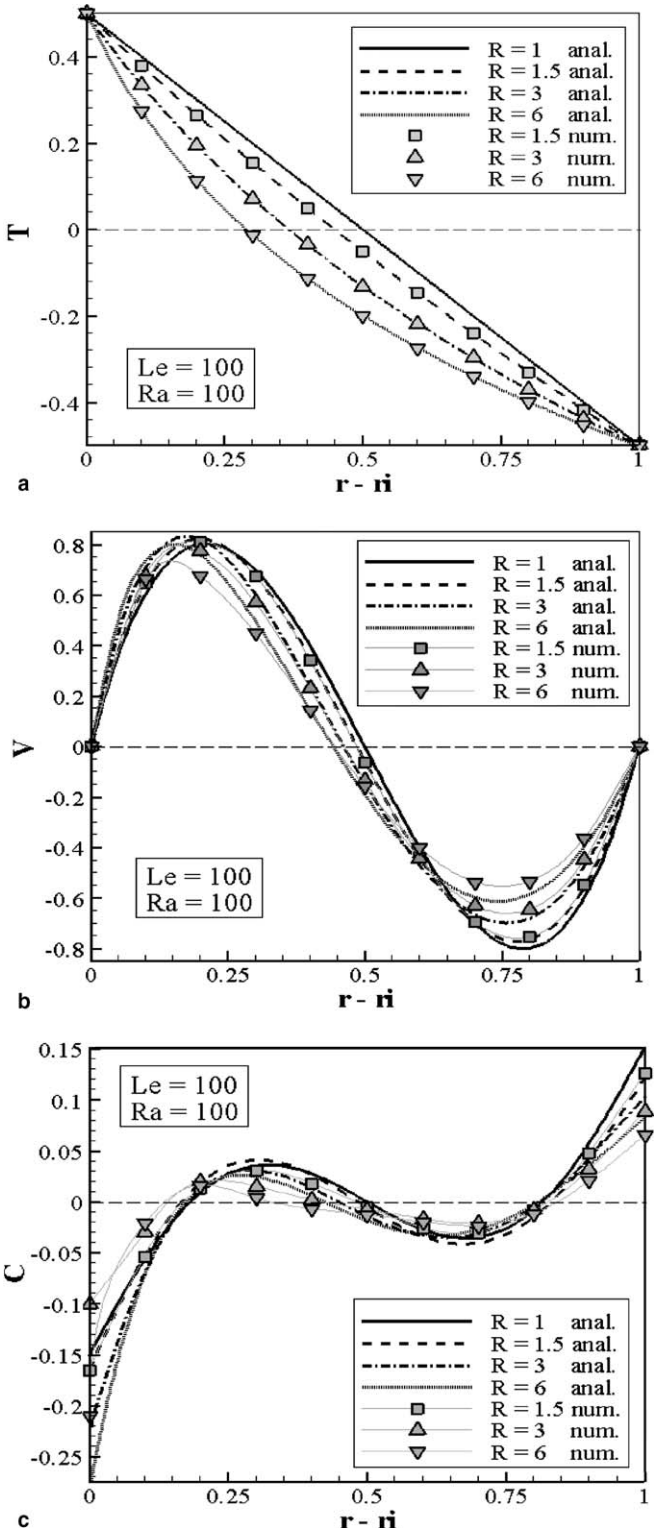

Fig. 4. Comparisons of the analytical and numerical results at different radius ratios at $\theta = 0$ and for $Ra = 100$ and $Le = 100$: (a) temperature, (b) velocity and (c) concentration fields.

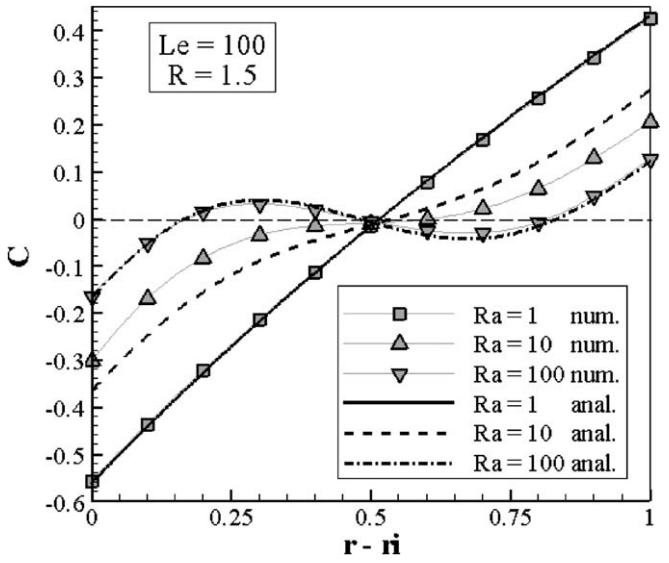

Fig. 5. Comparisons of the analytical and numerical concentration profiles evaluated at $\theta = 0$ for different Ra ($Le = 100$, $R = 1.5$).

radius ratio, as it happens to the numerical profiles. The influence on the profiles of the Rayleigh number, for fixed R, is mainly limited to the concentration. In fact, variations of Ra do not modify the temperature profile and cause only amplitude variations of the velocity.

The concentration profile is, on the other hand, quite sensitive to the value of Ra, as it can be observed in Fig. 5; for sufficiently high Ra, in fact, the natural convective motion causes the birth of an entrainment region that does not exist at low Ra, where the concentration profile is closer to the case of pure thermodiffusion ($Ra = 1$). From Fig. 5 it is possible to observe that the maximum mismatch between the analytical and numerical solutions occurs for $Ra = 10$, i.e. in the range of Ra for which the formation of the entrainment region is observed, as a consequence of simplifying assumptions introduced in the derivation of the analytical solution.

It is possible to notice that for sufficiently low values of the Rayleigh number, which is the usual condition for the observation of this kind of phenomena, the agreement between the analytical and numerical results is, in the overall, satisfactory. When Ra increases, two kind of phenomena may occur, depending on the value of the radius ratio. In particular, for high values of R the concentration field presents a plume that tends to disrupt the stratified distribution, whereas, for low values of R the temperature and velocity distributions are characterised by a multicellular regime [5,6], enhancing the mixing and avoiding compound separation.

The possibility to separate the components of a binary mixture filling a cavity is a phenomenon of primary importance for the application of thermogravitation. It is therefore necessary its full exploitation for the system herein considered.

The concentration profiles reported in Fig. 2 show that the stationary state is characterised by the existence of accumulation regions in which the mixture components are more concentrated. These regions are located around the vertical axis, respectively at the bottom of the cavity

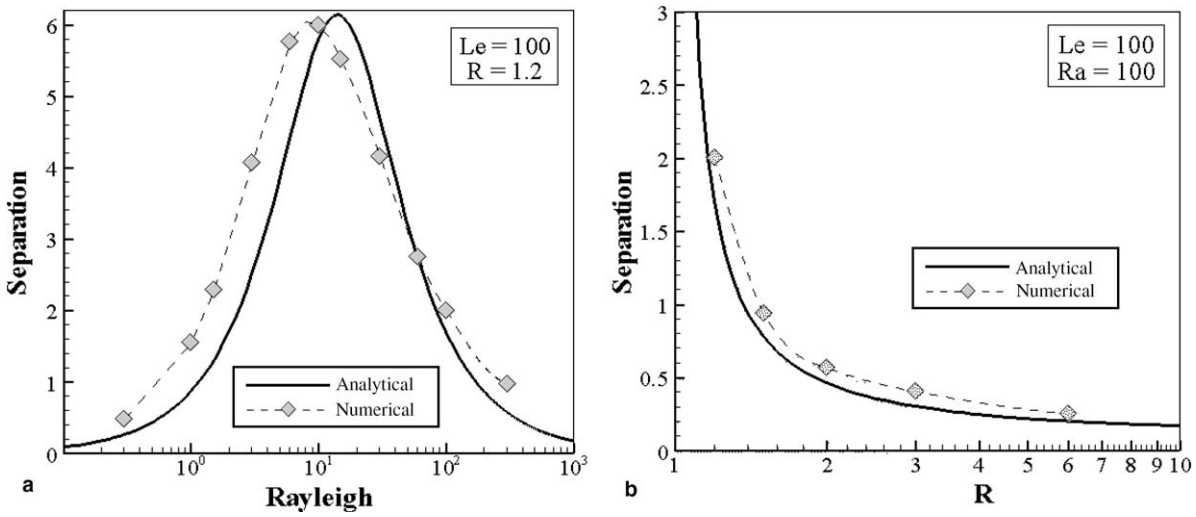

Fig. 6. Analytical and numerical evaluation at $Le = 100$ of the dependence of compound separation on: (a) Ra, for $R = 1.2$, and (b) R, for $Ra = 100$.

in contact with the external cylinder for the heaviest component and at the top of the cavity in contact with the internal cylinder for the lightest component. The separation of the two components is therefore globally characterised by an azimuthal variation. Under these conditions, the analytical solution previously defined allows to easily calculate the separation, s, according to

$$s = C|_{\theta=-\pi/2} - C|_{\theta=+\pi/2} = -2b\pi \tag{27}$$

It is important to analyse, for a specified mixture, the influence of the Rayleigh number and of the radius ratio on the separation. Fig. 6 reports, for $Le = 100$, the dependence of both the analytical and numerical separation on Ra (plot (a)) and on R (plot (b)). The analysis of plot (a) points out the existence of an optimal value of Ra leading to maximum separation of the mixture compounds in an annular cavity; moreover, this value is predicted with satisfactory approximation by means of the analytical solution. This result is similar to what has been found for rectangular cavities [2], where separation has been found to correspond to a rational fraction of the non-dimensional group $Ra\,Le$.

This result is fundamental as it allows to determine, for example, the optimal gap of a cavity designed for achieving efficient compound separation. The application to the previous case of mixture of water and isopropanol with $R = 1.5$, gives

$$s_{\max} = 4.097 \quad \text{for } Ra_{\text{opt}} = 9.71 \quad \text{and} \quad e = 0.353 \ \text{mm}$$

The analysis plot (b) points out that the growth of the radius ratio causes the decrease of compound separation and, by extrapolation, the most appropriate configuration for enhancing the separation is the rectangular geometry.

5.2. Pure fluids

As mentioned earlier, for the case of pure fluids the interest is focused on the capability of the analytical model to predict the heat transfer. Therefore, the comparison of the analytical and numerical Nusselt number has been performed to assess the validity of the analytical solution in a range of Ra values for which the pseudo-conductive regime was numerically observed. In particular, comparisons has been performed by varying R for fixed $Ra = 1500$, and then by varying Ra for $R = 1.2$. The following variables have been considered for comparisons:

- radial temperature profile, at $\theta = 0$, $T(r;0)$,
- radial profile of the tangential velocity at $\theta = 0$, $v(r;0)$,
- global Nusselt number.

Fig. 7 reports the comparisons of the analytical and numerical $T(r;0)$ and $v(r;0)$, respectively in the first and second column, evaluated at $Ra = 1500$ and for: $R = 2.60, 2.00, 1.60, 1.20, 1.12$.

From the analysis of this figure it is possible to observe how the fitting of the analytical and numerical solution, relatively poor for $R = 2.60$, rapidly improves with the reduction of R. Indeed, the numerical profiles are satisfactorily predicted by the analytical model for $R = 1.6$. This result depends on the simplifying assumption of pseudo-conductive regime introduced in the derivation of the analytical solution, which progressively loses validity for growing values of the radius ratio. The higher is R, in fact, the greater is the deformation of both temperature and velocity actual profiles with respect to the assumed pseudo-conductive profiles.

The global Nusselt number, Nu, has been defined using the following relations [6]:

$$\begin{aligned} \overline{Nu_{\text{i}}} &= -\frac{r_{\text{i}} \ln R}{2\pi} \int_0^{2\pi} \left(\frac{\partial T}{\partial r}\right)_{r=r_{\text{i}}} \mathrm{d}\theta \\ \overline{Nu_{\text{e}}} &= -\frac{r_{\text{e}} \ln R}{2\pi} \int_0^{2\pi} \left(\frac{\partial T}{\partial r}\right)_{r=r_{\text{e}}} \mathrm{d}\theta \end{aligned} \tag{28}$$

where subscripts "i" and "e" refer respectively to the internal and external cylinders. For the particular case of

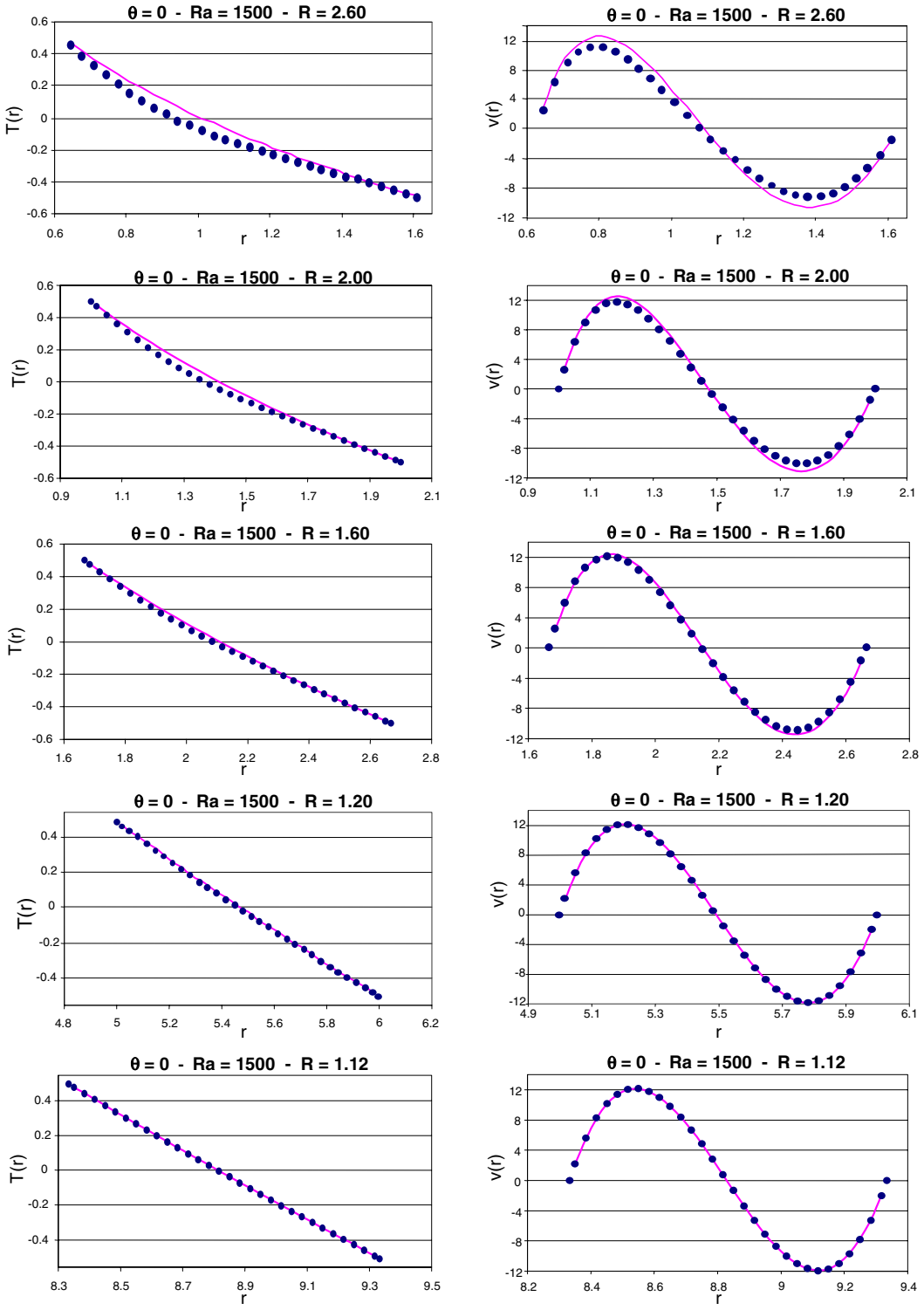

Fig. 7. Analytical (full line) and numerical (dots) profiles at $\theta = 0$ for $Ra = 1500$ and various R: temperature $T(r)$ (left-hand column) and velocity $v(r)$ (right-hand column).

stationary behaviour, verified in the numerical model for $Ra = 1500$ and for all of the values of R herein considered, it is easy to verify that

$$\overline{Nu_i} = \overline{Nu_e} = \overline{Nu} \tag{29}$$

In the analytical solution, deriving the temperature profile expressed by Eq. (20) and substituting in one of Eq. (28), $Nu = 1$ is found for any value of R. This is an expected result as a consequence of the assumption of pseudo-conductive regime used to build the analytical

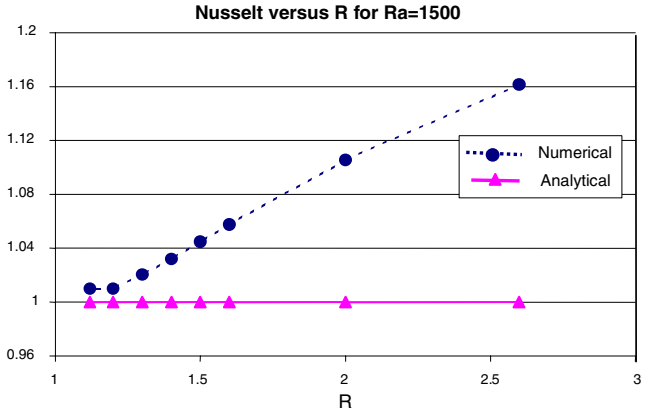

Fig. 8. Nusselt number versus R calculated for $Ra = 1500$.

model. On the other hand, in the numerical model the actual temperature profile is considered, leading to a dependence on R of the Nusselt number.

Fig. 8 shows the comparison between the analytical and numerical Nusselt number. It is possible to observe that for $R = 1.4$ the error of the analytical model is below 3%, which can be considered an acceptable prediction for most applications. The upper value of R can therefore be assumed as upper limit for the validity of the analytical solution.

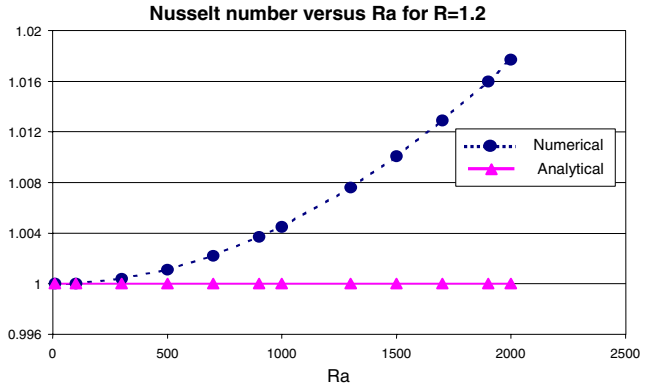

Fig. 9. Nusselt number versus Ra calculated for $R = 1.2$.

On the basis of this result, the following comparisons have been performed for $R = 1.2$ (for which the error on Nu is below 1%), in order to determine the range of Ra in which the analytical model performs satisfactorily.

Fig. 9 shows the analytical and numerical Nu calculated for $R = 1.2$ and Ra varying between $Ra = 1$ and 2000. It can be seen that the analytical solution satisfactorily predicts the Nu number within the whole range of Ra, with a maximum error below 2% at $Ra = 2000$.

It is worth noting also that, as reported in Fig. 10(a) and (b), a strict fit has been obtained between the analytically and numerically profiles evaluated at $\theta = 0$ for all of the values of Ra considered, both for the temperature (where the various profiles are superimposed) and for the tangential velocity.

No further increase has been considered with respect to $Ra = 2000$ since for $R = 1.2$ a bifurcation occurs at $Ra = 2130$. This bifurcation is of the Rayleigh–Bénard type and occurs through the birth of two small cells at the top of the annulus, separating the two counterotating cells formerly occupying the whole cavity [10]. Due to the bifurcation, the initial assumption of the existence of two counterotating cells, on the basis of which the analytical solution has been defined, loses its validity. Similar results can be obtained for other values of R, each of which is characterised by a critical value of Ra where the above mentioned bifurcation occurs and the analytical model looses its validity. The calculation of the critical values of Ra at various R is beyond the scope of the present study, mainly devoted to presenting an analytical solution for the pseudo-conductive regime, and will be developed in future numerical studies.

6. Conclusions

In this study an analytical model has been defined for the description of the thermal–fluidynamic behaviour of either a binary mixture or a pure fluid filling a horizontal annular cavity isothermally cooled outside and heated inside. The case of binary mixture is complicated by the occurrence of thermogravitational diffusion, due to the

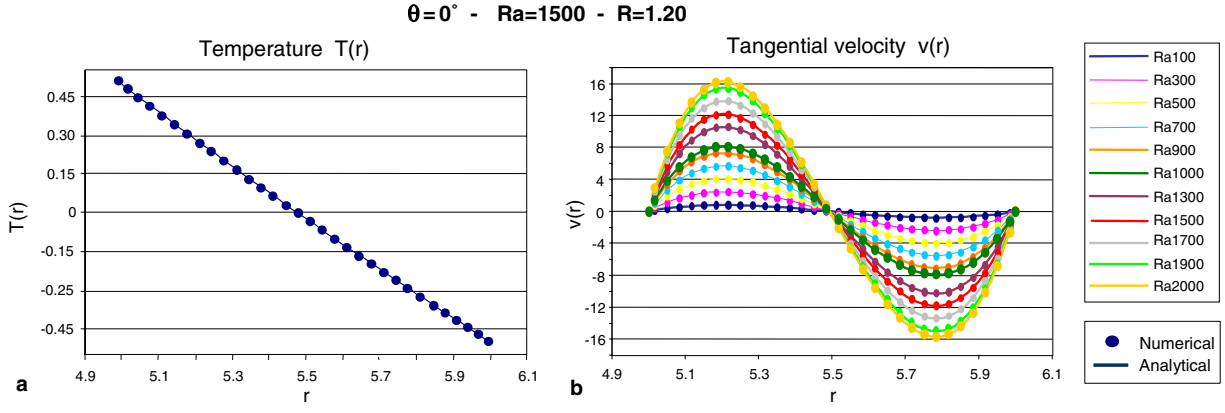

Fig. 10. Analytical versus numerical profiles at $\theta = 0$, $R = 1.2$ and Ra varying between $Ra = 1$ and 2000: (a) temperature $T(r)$ and (b) radial component of tangential velocity $v(r)$.

coupling between natural convection and thermodiffusion in presence of a temperature gradient. This effect produces the separation of the mixture compounds. Nonetheless, the study shows that neglecting the additional buoyancy term generated by the existence of a concentration gradient allows to decouple the momentum and energy equations from the concentration equation. In this way, the model for binary mixtures is made up of two submodels.

The first submodel consists of the coupled energy and momentum equations and is mathematically equivalent to the case of pure fluids. An analytical solution for the velocity and temperature profiles has been obtained from this submodel for the case of pseudo-conductive regime, which is typical at values of *Ra* below a critical value dependent on the cavity radius ratio.

The second submodel simply consists in the concentration equation and can be integrated once that the analytical velocity profile has been determined from the integration of the previous submodel.

The analytical model has been validated through several comparisons. For the case of binary mixtures, particular attention has been devoted to verify the capability of the analytical model in estimating the separation of the mixture compounds inside the cavity, which occurs only for low *Ra* values. For the case of pure fluid the focus has been in the validation of the analytical model within the range of *Ra* values for which the pseudo-conductive regime exists.

References

[1] W.H. Furry, R. Clark Jones, L. Onsager, On the theory of isotope separation by thermal diffusion, Phys. Rev. 55 (1939) 1083–1095.
[2] M. Marcoux, M. Hammoudi, G. Desrayaud, G. Lauriat, Etude de la diffusion thermogravitationelle dans un mèlange deux o trois constituants, Congrès SFT, 2001, pp. 241–246.
[3] M. Marcoux, M. Hammoudi, G. Desrayaud, Etude de la convection thermosolutale dans une cavité annulaire verticale, Congrés SFT, 2002, pp. 237–242.
[4] M. Marcoux, M.C. Charrier-Mojtabi, M. Azaiez, Double-diffusive convection in an annular vertical porous layer, Int. J. Heat Mass Transfer 42 (1998) 2313–2325.
[5] R.E. Powe, C.T. Carley, E.H. Bishop, Free convective flow patterns in cylindrical annuli, J. Heat Transfer 91 (1969) 310–314.
[6] G. Desrayaud, G. Lauriat, P. Cadiou, Thermoconvective instabilities in a narrow horizontal air-filled annulus, Int. J. Heat Fluid Flow 21 (2000) 65–73.
[7] R.E. Powe, C.T. Carley, S.L. Carruth, A numerical solution for natural convection in cylindrical annuli, J. Heat Transfer 93 (1971) 210–220.
[8] Y. Rao, Y. Miki, K. Fukuda, Y. Takata, S. Hasegawa, Flow patterns of natural convection in horizontal cylindrical annuli, Int. J. Heat Mass Transfer 28 (1985) 705–714.
[9] C.J. Kim, S.T. Ro, Numerical investigation on bifurcative natural convection in an air-filled horizontal annulus, in: Proc. 10th Int. Heat Transfer Conf., vol. 7, 1994, pp. 85–90.
[10] P. Cadiou, G. Desrayaud, G. Lauriat, Natural convection in a narrow horizontal annulus: the effects of thermal and hydrodynamic instabilities, ASME J. Heat Transfer 120 (1998) 1019–1026.